Polymer 50 (2009) 4706–4717

Contents lists available at ScienceDirect

Polymer

journal homepage: www.elsevier.com/locate/polymer

Single- and double-ring spherulites in poly(nonamethylene terephthalate)

E.M. Woo*, Yu-Fan Chen

Department of Chemical Engineering, National Cheng Kung University, Tainan 701-01, Taiwan

ARTICLE INFO

Article history:
Received 3 April 2009
Received in revised form
24 July 2009
Accepted 25 July 2009
Available online 29 July 2009

Keywords:
Poly(nonamethylene terephthalate)
Ring band
Thin film

ABSTRACT

A new mechanism of formation of ring-banded spherulites was discovered, where three different types of spherulites were present in poly(nonamethylene terephthalate) (PNT) cast in thin film forms. The growth and morphological features in three ring-banded spherulites were compared and analyzed using polarized/non-polarized light microscopy, differential scanning calorimetry (DSC), and scanning electron microscopy (SEM) and element analysis by energy dispersive spectroscopy (EDS) on surfaces of spherulites. Three types of spherulites (labeled: Type-0, 1, and 2) are possible in PNT when crystallized at wide range of crystallization temperature (T_c); however, only two of the three types can co-exist in PNT at a given T_c. At lower T_c (<55 °C), within Regime-III, the spherulites in PNT are either of Type-0 (appearing ringless in POM) or Type-2 (double-band in POM). When crystallized at temperature of $T_c = 55$ °C or higher (Regime-II), the morphology is featured with Type-1 (single-ring-banded in POM) spherulites as the majority species that co-exist with Type-2 (double-ring-banded in POM) spherulites as imbedded minority. Origins and morphological differences of the single-band vs. double-band spherulites were compared. The double-band spherulites have much larger inter-ring spacing than do the single-band spherulites. By comparison, the rod-like lamellae in the double-banded spherulites (Type-2) are longer and thicker, and more ordered than those in the single-banded spherulites (Type-1).

1. Introduction

Spherulitic morphology in semicrystalline polymers has been widely studied in past decades. Typically, Maltese-cross type spherulites are most common. Under certain conditions (crystallization temperature (T_c), diluents, film thickness, etc.), some semicrystalline polymers in thin film forms are known to exhibit several interesting spherulitic patterns, such as ring-bands and dendritic types. Ring-banded spherulites have been known to exist in certain semicrystalline polymers in film forms when crystallized at certain conditions. Some classical vinyl polymers (e.g., polyethylene; or poly(vinylidene fluoride)) [1–4] may show typical Maltese-cross pattern as well as ring-banded spherulites, respectively, when crystallized at different T_c. Such examples of rings in spherulites can also be seen in several aryl-polyesters or other semicrystalline polymers [5–13]. Ring-bands and mechanisms of their formation have been widely discussed in the literature [14–25]. Lotz and Cheng [24] in a review article with many references cited therein have comprehensively addressed twisting of polymer lamellae with appearance of concentric bands (i.e., ring-bands) in spherulites. They have clarified in depth many structural features related to ring-bands in polymers; nevertheless, the variety of factors influencing ring patterns in polymers (or blends) may still challenge many future investigators.

The issues are further complicated as the mechanisms for ring band formation might not be universal. The mechanism of ring-bands for one polymer might be different from that for other polymers. An earlier study has revealed that in the ring-band crystal region of poly(butylene adipate) (PBA) [26], the lamellar stalks, tapering off to pointed needle-like stalk, monotonously protrude out of layers of softer materials, with no signs of twisting, bending, or turning. Wang et al. [27,28] have proposed that the concentric rings in the birefringent ring-banded spherulites, as well as those in the nonbirefringent ring-banded spherulites, are a manifestation of periodic variation of thicknesses along the radius for poly(ε-caprolactone) (PCL) grown from solution. The development of the variation of thicknesses is due to periodic diffusion-induced rhythmic growth associated with the change of concentration gradient in polymer solution with constant concentration via the control of solvent evaporation rate during the spherulite growth in PCL solution. Other investigators propose yet different mechanisms for ring-bands in chiral polymers. A relationship between the molecular chirality of poly(lactide)s (PLA) and their macroscopic behavior is established by Maillard and Prud'homme [29], where they have

* Corresponding author. Tel.: +886 6 275 7575x62670; fax: +886 6 234 4496.
E-mail address: emwoo@mail.ncku.edu.tw (E.M. Woo).

0032-3861/$ – see front matter © 2009 Elsevier Ltd. All rights reserved.
doi:10.1016/j.polymer.2009.07.040

shown that edge-on lamellae are present in PLA, showing a curvature related to polymer chirality, in ultrathin films (~15 nm) by using a forced nucleation technique. The direction of curvature of the lamellae can be linked with the sense of twisting of the PLA lamellae in ring-banded spherulites, and the temperature-dependent radius of curvature can be correlated to the distance between extinction rings. Formation of ring-bands in polymer blends has also been widely studied in comparison to neat polymers. Chen and Yang have proposed that for crystalline polymer blends of poly(aryl ether ketone) (LC-PAEK) and poly(aryl ether ether ketone) (PEEK), the formation of ring-banded spherulites is attributed to structural discontinuity caused by rhythmic radial growth [30]. The view of structural discontinuity, apparently, is quite dramatically in contrast with other prevailing proposals that ring-bands are a result of coordinated lamellar twisting. Blend of poly(ε-caprolactone) (PCL) and poly(vinyl chloride) (PVC) with 90 wt% PCL was examined by Cheung et al. [31], where they have concluded by time-of-flight secondary ion mass spectrometry (ToF-SIMS) that the distribution of Cl of PVC on the concentric rings is caused by the change in the surface morphology as PCL lamellae twist along the radial growth. Amorphous PVC is segregated on the valleys that consist of PCL flat-on lamellae, and semicrystalline PCL is on the ridges that consist mainly of edge-on lamellae. These various studies point out that ring-bands can be of many different types, and the ring band in variously different types of polymers (or blends) may involve complex and possibly different mechanisms, where no simple or uniform rules govern formation of ring-bands.

However, there are still a lot of issues remaining yet unresolved. It is generally reported that only a single type of spherulite pattern is present in polymers. Under some conditions, co-existing ring-banded and ringless spherulites can be present [32]. Why, in a same polymer, two different types of spherulites (ringless and ring-banded) are present? Under polarized light, it is known that patterns of ring-bands in spherulites can be sub-divided into two types: single- and double-ring bands [33]. What are differences between the single- and double-ring-banded spherulites? Many other problems have yet to be resolved. What is the fine morphological difference between the single and double bands? To answer these intellectually probing questions, this study synthesized, examined the crystal structures and spherulite morphology in poly(nonamethylene terephthalate) (PNT), which has 9 methylene units (odd numbered) between two terephthalates. Note that polymorphism can be present in PNT according to preliminary characterization. But when melt-crystallized at any T_c, there is only one crystal form, and the only additional different crystal form is possible when PNT is solvent-crystallized. However, such polymorphism issues were not main objective of this study. This study focused on interesting dual ring-banded structures, single-ring and double-ring-banded spherulites, in PNT that had been less studied owing to lesser commercial interests.

2. Experimental

2.1. Materials

Poly(nonamethylene terephthalate) (PNT), with 9 methylene units between two terephthalate groups, was synthesized by two-step crystallization via transesterification and polycondensation by using 1,9-nonanediol and dimethyl terephthalate with 0.1% butyl titanate as a catalyst. The weight-average molecular weight (M_w) and the polydispersity index (PDI) as determined by gel permeation chromatography (GPC, Waters) were 32,700 g/mol and 1.44, respectively. PNT was purified several times after synthesis prior to use. Preliminary characterization revealed that $T_g = 0.1$ °C and $T_m = 91.6$ °C. Structure of PNT is shown as follows:

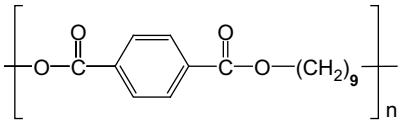

A solution prepared of a proper amount of purified PNT by dissolving in chloroform (~2 wt%), which was then cast on glass slides or polyimide films for polarizing optical microscopy (POM) and scanning electron microscopy (SEM) observations. After solution casting and proper drying, the PNT cast films on glass were briefly melted to liquid at ~120 °C, and then rapidly brought to an isothermal $T_c = 40$–85 °C for full crystallization. Film thickness after subtracting the glass slide was estimated to be ca. ~5–10 μm.

2.2. Apparatus and procedures

2.2.1. Thermal transition and crystallization rate

Glass-transition temperature (T_g) transitions of the blend samples were measured with a differential scanning calorimeter (DSC-7, Perkin–Elmer) equipped with an intracooler (to −60 °C) and data acquisition/analysis. Prior to DSC runs, the temperature and heat of transition of the instrument were calibrated with indium and zinc standards. During thermal annealing or scanning, a continuous nitrogen-gas flow in the DSC sample cell was maintained to ensure minimal sample degradation.

2.2.2. Morphology characterization

Polarizing optical microscopy (POM, Nikon POL-2) and a Nikon DS-5M-U CCD digital camera were used to observe the morphology and the growth rate of PNT spherulite. Thin films for polarizing optical microscopy (POM) were obtained by casting polymer solution on one side of glass slides at 45 °C. A drop of 2% solution of the polymer in chloroform was deposited and uniformly spread on a glass slide and the solvent was allowed to fully evaporate in an atmosphere. The dried film sample was heated to the molten/liquid state for a short time and then rapidly cooled to the intended crystallization temperature (T_c) ranging from 40 to 80 °C. POM was used to investigate the spherulitic morphology of isothermally crystallized samples.

2.2.3. Growth rate measurements

Radial growth of spherulites was recorded and rates measured using a polarizing optical microscopy (POM, Nikon Optiphot-2) equipped with a temperature-controlled hot stage and a Nikon charge-coupled-device CCD digital camera and automatic image processing software. Magnification and scales were automatically calibrated by the software. Spherulite growth kinetics was based on samples of thin films (5 μm or less) on glass substrates. The growth rates below 40 °C were found to be too fast to be accurately recorded. Both polarized and non-polarized graphs of spherulites were recorded for comparison; furthermore, estimation of inter-ring spacing was also done using SEM graphs to be discussed later. This is especially critical for estimating the inter-ring band width in the spherulites showing ring-bands, as the ring spacing estimated from polarizing optical micrographs alone may be misleading.

2.2.4. Scanning electron microscopy (SEM)

Greater magnifications revealing the morphologies of PNT samples were also characterized at for comparisons using scanning electron microscopy (SEM, FEI Quanta 400F, and SEM, Philips XL-40 FEG). Washed/dried samples in film forms cast on glass slide substrates, after proper thermal treatments, were coated with vapor-deposited gold using vacuum sputtering prior to SEM characterization.

For discerning any elemental differences across the ridges and valleys of ring-bands, elemental analysis along radial direction across the ridge and valley of ring-bands was performed by energy dispersive spectrometry (EDS) (EDAX Genesis, attachment to SEM instrument).

3. Results and discussion

3.1. Isothermal growth rates of spherulite (based on Type-0 and Type-1 spherulites)

Radii of spherulites of PNT were measured as functions of time (t) at several isothermal temperatures (T_c between 37 and 77 °C, for 10 intervals). The slopes of straight lines yielded growth rates. With only slight deviation/scattering, the growth rates roughly follow a linear dependence on time. Fig. 1 shows the spherulite growth rates of Type-1 spherulites plotted as a function of T_c (isothermal temperature of crystallization). Type-2 spherulites are too few to be observed for thin films crystallized on glass slides. Only some growth rate data of Type-2 spherulites observed for a certain T_c's are discussed later in this study. The growth rate of Type-1 spherulite of PNT decreases with increasing T_c. The slopes of the straight lines yield rates of two-dimensional growth (μm/min) of the spherulites at the given T_c. At $T_c < 37$ °C (large degree of supercooling), the rates were too high with high nucleation, forming tiny spherulites. Thus, rates could not be measured for $T_c < 37$ °C. Attention is drawn to make a comparison between PNT and poly(octamethylene terephthalate) (POT) investigated earlier [34]. By comparison, at the same driving force of supercooling (ΔT), the growth rates for PNT are lower than those for poly(octamethylene terephthalate) (POT) [34]. The odd number of methylene segments in the structure of PNT may be responsible for the noted slower rates. It appears that regime transition occurs at some intermediate T_c. To analyze the regime behavior of spherulite growth, treatments according to the Lauritzen–Hoffman secondary nucleation theory, which is expressed as following [35]:

$$G = G_o \exp\left[\frac{-U^*}{R(T_c - T_\infty)}\right] \exp\left[\frac{-K_g}{T_c(\Delta T)f}\right] \quad (1)$$

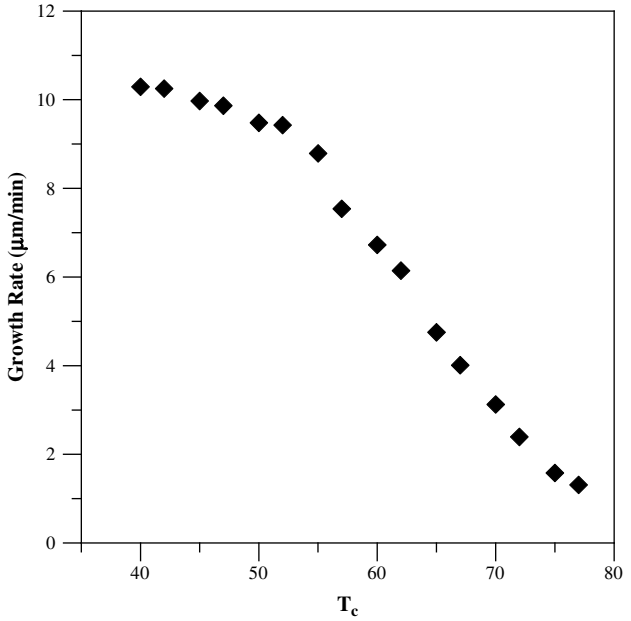

Fig. 1. Plot of growth rates vs. T_c's of PNT.

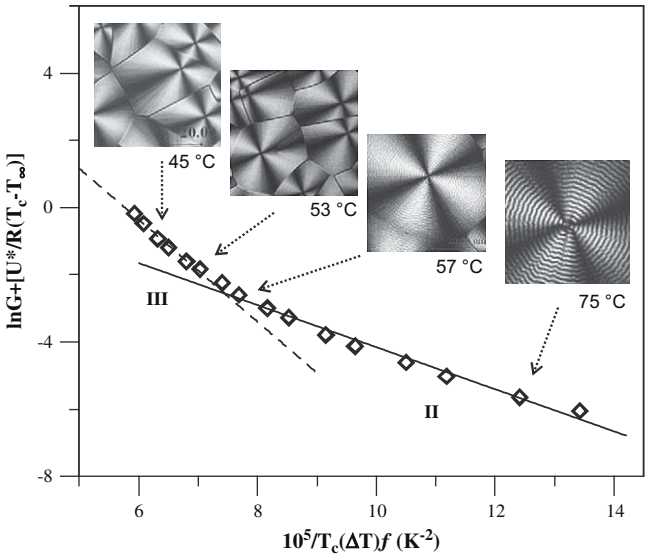

Fig. 2. Lauritzen–Hoffman plot of PNT with $U^* = 1500$ cal/mol. Insets: spherulite patterns at corresponding T_c in Regimes-II and -III, with $T_{III \to II} = 55.4$ °C.

where G is the radial growth rate, G_o is an overall constant that depends on molecular weight, and U^* is the activation energy. $T_\infty = T_g - 30\ K$ is the temperature at which diffusion stops, which denotes the degree of under-cooling, and $f = 2T_c/T_m^o + T_c$. The f factor is a correction coefficient for the temperature dependence of enthalpy of fusion. K_g is the nucleation constant, which can be obtained from $K_g = n_e b_o \sigma \sigma_e T_m^o / \Delta H_f^o{}_K$. The procedures are classically standard and thus not discussed in details here. Equilibrium melting temperature ($T_m^o = 98.9$ °C) of PNT was obtained from extrapolation by the classical Hoffman–Weeks method, and ΔH_f^o is the enthalpy of fusion per unit volume of a perfect and infinitely large crystal at its T_m. For $U^* = 1500$ cal/mol, $K_g(III)/K_g(II) = 2.16$ is resulted, which is close to the theoretical value of 2.0 according to the predictive requirement of $K_g(III) = 2\ K_g(II)$.

Fig. 2 shows the Lauritzen–Hoffman plot of PNT. Inset graphs show the spherulite patterns found at corresponding T_c in regimes-II and -III, respectively. For $T_c = 37$–53 °C (Regime-III), PNT spherulites exhibited almost no or very few ring-band spherulites but primarily ringless ones with Maltese-cross as the major species; for $T_c = 55$–77 °C (Regime-II), apparent ring patterns were seen in most PNT spherulites. Temperature at the discontinuity (i.e., transition from Regime-II to -III) is located at near 55 °C ($T_{II \to III}$). The two

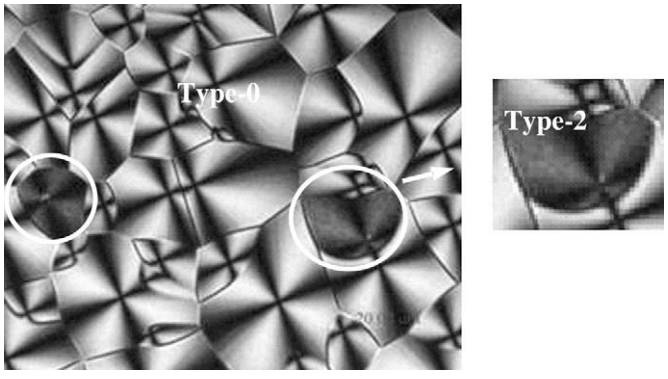

Fig. 3. POM photographs for PNT melt-crystallized at 45 °C, showing two co-existing types of spherulites. Crystals in circles showing minority spherulite pattern (Type-2 double ring-bands) surrounded by majority spherulite pattern (Type-0, ringless Maltese-cross).

intersecting lines yield a point of transition at $T_{III \rightarrow II} = 55.4\ ^{\circ}C$. The ringed spherulites in this regime can be sub-divided into two types, single- and double-ring, which will be further discussed later. $T_c = 55\ ^{\circ}C$ seems to be the point of discontinuity where spherulite patterns display a change. Within Regime-II ($T_c = 55$–$77\ ^{\circ}C$), the inter-ring distance between two neighboring concentric/spiraling rings in PNT spherulites was found to be dependent on temperature. Each of the concentric/spiraling ring-bands in spherulites apparently becomes thickened with an increase in temperature of crystallization (T_c). Inter-ring distance (band width) increases with T_c, too, which will be quantitatively correlated with T_c in later discussions.

3.2. Dual spherulite-types in PNT crystallized at T_c

Fig. 3 shows spherulites of PNT melt-crystallized at 45 °C, displaying two types of spherulites, i.e., ringless and ring-banded types. The ring-banded spherulite, on closer inspection and at larger magnifications, actually appeared as double-ring-banded using POM, and is therefore labeled as "Type-2". The Type-2 ring-banded spherulite appears as a minority species in comparison to the major and dominating Type-0 spherulites. Thus, these two co-existing spherulite-types in PNT crystallized at $T_c = 45\ ^{\circ}C$ are hereby termed as Type-0 and Type-2, respectively, indicating ringless and double-ring-banded spherulitic patterns. Interestingly, two types of

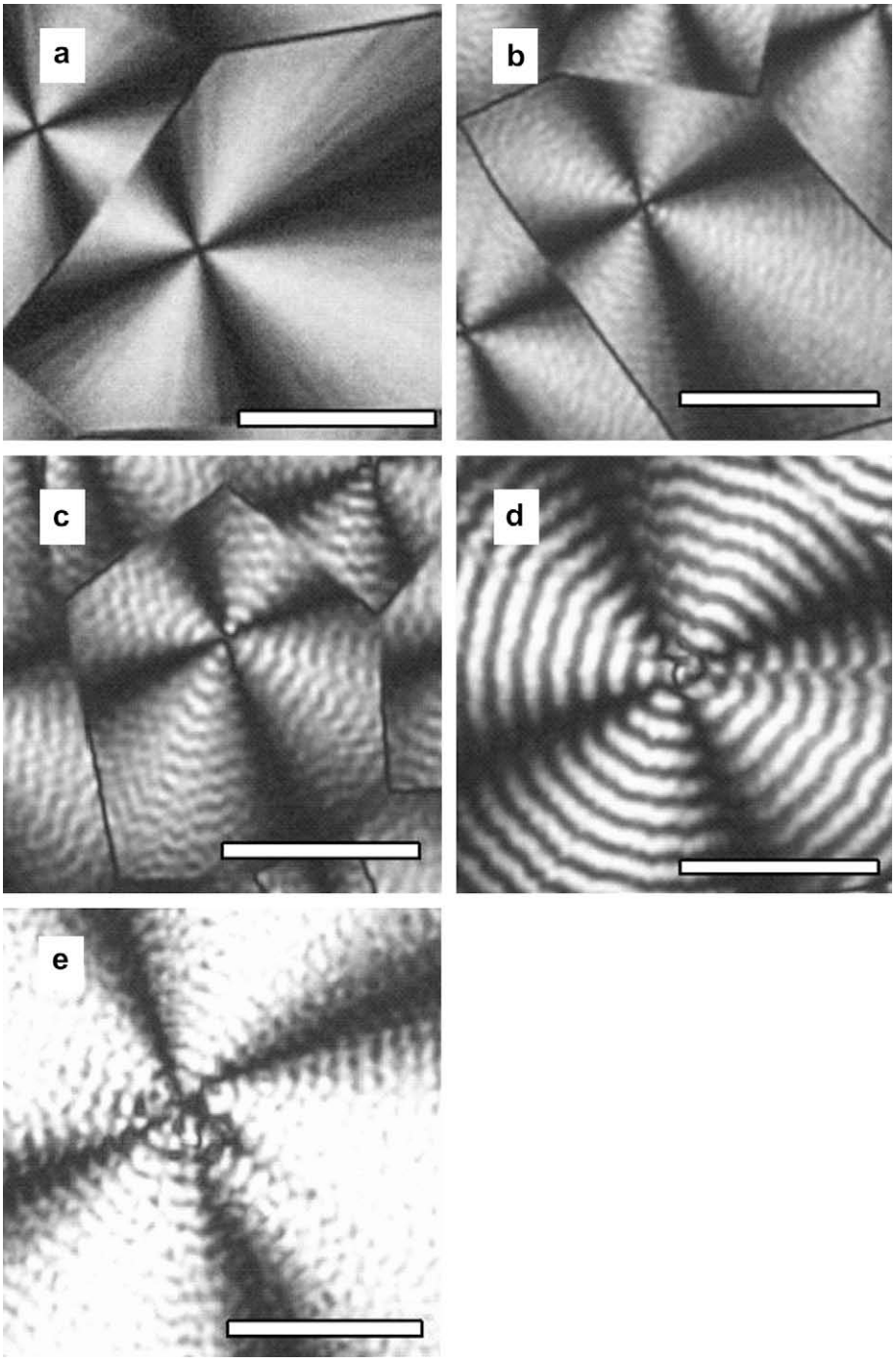

Fig. 4. POM micrograph for PNT Type-0 and Type-1 spherulites grown at various T_c: (a) 45, (b) 55, (c) 60, (d) 70, and (e) 80 °C. Scale bar = 20 μm.

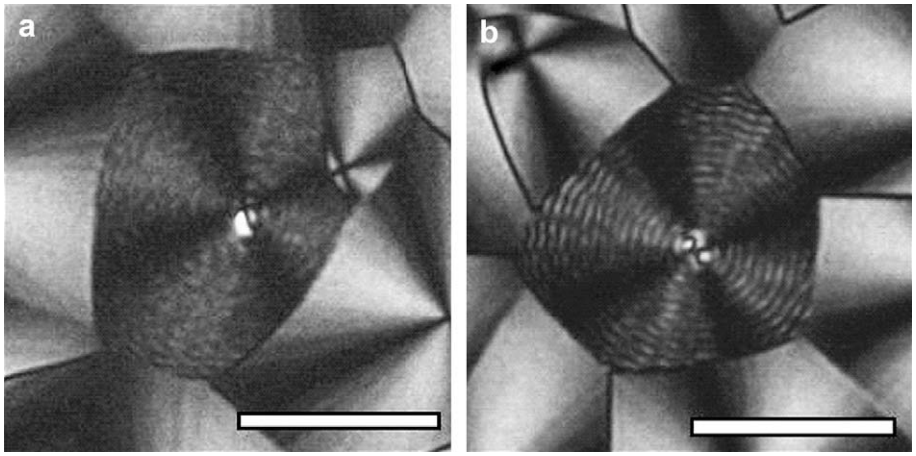

Fig. 5. POM photos for the melt-crystallized PNT showing majority Type-0 spherulites (ringless) with minority imbedded Type-2 (double-ring-banded) spherulites at low $T_c =$: (a) 45, and (b) 50 °C.

spherulites are clearly seen in PNT film samples crystallized at the low temperature of 45 °C, where the crystallization rate was considerably higher (in comparison to those at 70 °C or higher). Crystals in the circles show different patterns (double-ring-banded type) from the surrounding area (ringless Maltese-cross type). Apparently, at $T_c = 45$ °C, Type-0 (ringless/Maltese-cross) is the majority while Type-2 (double-ring-banded type) is minority. Thus, dual types of spherulites (ringless vs. ring-banded) of various relative fractions co-exist in PNT crystallized at any temperatures of crystallization. Alternatively, in PNT crystallized at higher T_c (greater than $T_i = 55$ °C), single-ring-banded spherulites (Type-1), replacing Type-0 spherulites, becomes the major species.

3.3. Ringless, single-band, and double-band spherulites

As discussed earlier, two regions of growth leading to different types of spherulites (Type-0, Type-1, and Type-2) are apparent in PNT crystallized at 45–85 °C. At $T_c = 45$ °C, PNT develops a morphology

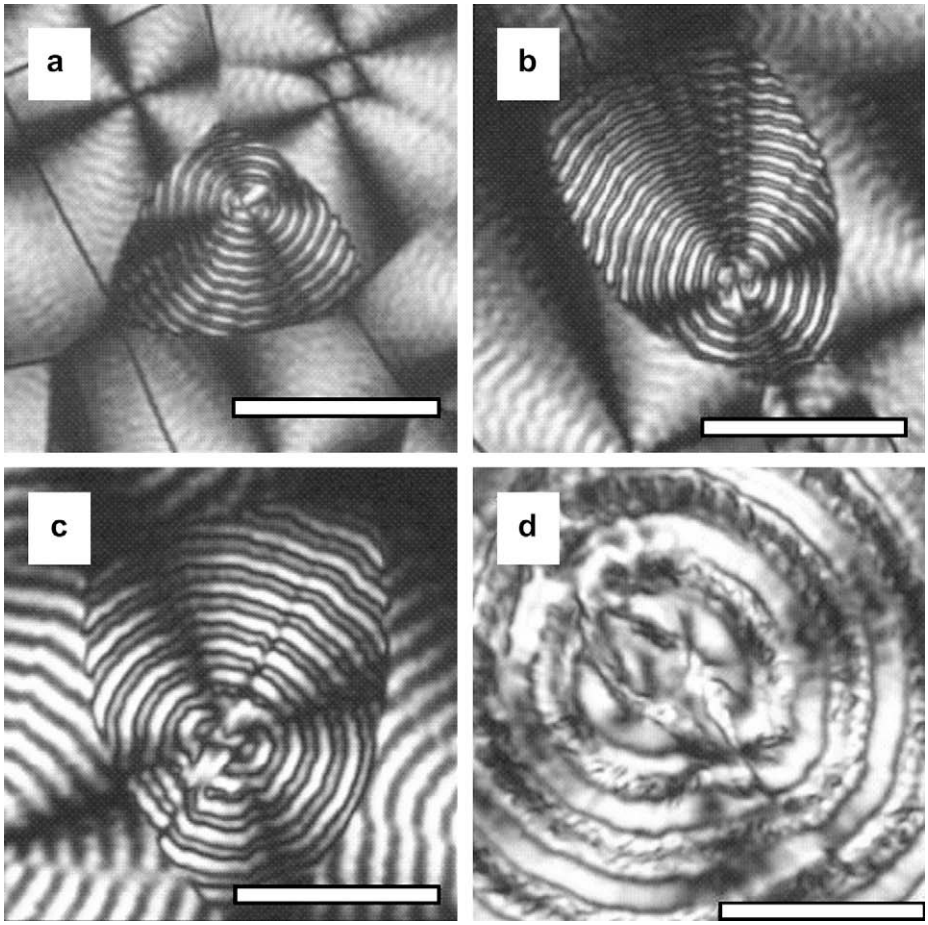

Fig. 6. POM photos for the melt-crystallized PNT showing majority Type-1 (single-banded) with imbedded minority Type-2 (double-banded) spherulites grown at higher $T_c =$ (a) 55, (b) 60, (c) 70, and (d) 80 °C. Scale bar = 20 μm.

with dual spherulites, where the double-ring-banded Type-2 (occluded minority) is surrounded by majority Type-0 (ringless) spherulites. However, the relative fractions of these two types in PNT do not change much with respect to T_c of crystallization; Type-2 (double-ring-banded) spherulites are always present in minority in comparison to the other type. Lower T_c like 40–45 °C, in contrast to higher T_c such as 75–85 °C, does lead to slightly higher probabilities of finding Type-2 (double-ring-banded) spherulites among the majority either Type-0 or Type-1 spherulites. This fact suggests that the Type-2 spherulites may be initiated by either heterogeneous or foreign nuclei and a careful comparison also indicates that the growth of Type-2 always lags behind that of Type-0.

The PNT samples grown at various T_c: (a) 45, (b) 55, (c) 60, (d) 70, and (e) 80 °C, were all characterized. Fig. 4 shows POM photos for Type-0 (ringless) or Type-1 (single-ring-banded) spherulite in PNT crystallized at (a) 45, (b) 55, (c) 60, (d) 70, and (e) 80 °C. At $T_c < 55$ °C, Type-0 (ringless as the majority) and minority Type-2 (double-ring-band) spherulites co-exist. At higher T_c, the single-ring-banded Type-1 replaces Type-0 (ringless) as the major species of spherulites that co-exist with minority Type-2 (double-ring-banded) spherulites. The POM evidence in this figure indicates that at $T_c > 55$ °C, Type-1 (single-ring-banded as majority) and Type-2 (minority and double-ring-band) co-exist in PNT. This figure only shows the POM photographs for Type-0 at lower T_c's or Type-1 spherulites at higher T_c's in PNT crystallized at various different T_c, and the minority Type-2 spherulites that are embedded in either dominating Type-0 or Type-1 spherulites will be discussed separately later. Note here that it is improper to state that the spherulite pattern can "change from original ringless to single-ring-banded pattern" with increase in temperature. The specific type of spherulites, once set in its pattern at a T_c, can only grow increasingly large with time, but will not change further in patterns upon heating to higher temperatures. It is, however, proper to claim that PNT crystallized at lower T_c (<55 °C) is featured with dual types of spherulites (Type-0 and Type-2); while PNT crystallized at higher T_c (>55 °C) is featured with different dual types of ring-banded spherulites (dominating Type-1 and minority Type-2).

Thus, $T_c = 55$ °C constitutes a borderline temperature, below or above which the majority spherulite species in crystallized PNT assumes a different ring-band pattern. At $T_c < 55$ °C, all spherulites in PNT are either Type-0 or Type-2 (double-ring-banded), but no sign of Type-1 spherulites is seen. $T_c = 55$ °C is a point of discontinuity for growth of spherulites in PNT, where the Type-0 (ringless) spherulite ceases to grow, but a new Type-1 spherulite type (single-ring-banded pattern) appears instead. That is, the Type-1 (single-ring-banded) spherulite species replaces Type-0 as the majority species at $T_c = 55$ °C or higher. Note that the Type-2 spherulites are present at all temperatures, but they are slower-growing and are always the minority species embedded among the dominating Type-0 or Type-1 spherulites.

To visually illustrate how the minority Type-2 spherulites are embedded in the majority Type-0 spherulites in PNT crystallized at T_c lower than 55 °C, Fig. 5 displays POM photos for the melt-crystallized PNT showing majority Type-0 spherulites with minority imbedded Type-2 (double-ring-banded) ones at lower T_c of (a) 45 and (b) 50 °C. Note that the POM photographs were taken by focusing on the few number of Type-2 spherulites; thus the photographs do not present the actual percentages of Type-2 vs. Type-0 spherulites. The double-ring Type-2 spherulites are scarcely present and are surrounded by the majority Type-0 spherulites. Although the POM photographs as shown in the figure may be somewhat insufficiently clear to reveal the morphological features, later discussions using SEM data will address the finer details of ring-bands.

At temperatures of $T_c = 55$ °C or higher, Type-1 (single-ring-banded) now replaces Type-0 as the majority species in crystallized PNT, and imbedded in the majority Type-1 is still the minority Type-2 (double-ring-banded) spherulites. Again, to illustrate how the Type-1 spherulites arrange themselves with the embedded Type-2 minority spherulites in PNT crystallized at higher T_c's (>55 °C), Fig. 6 shows POM photos for PNT melt-crystallized at various T_c: (a) 55, (b) 60, (c) 70, and (d) 80 °C. All micrographs show clearly that the majority Type-1 (single-band) with minority imbedded Type-2 (double-ring) spherulites co-exist in the PNT, with spherulite patterns of each type varying with respect to T_c. In general, with increasing T_c, the ring-bands thicken and inter-ring spacing increases. In addition to pattern differences, the Type-1 and Type-2 spherulites also differ in radial growth rates. Analysis by POM in situ monitoring at several isothermal temperatures shows that growth rates of Type-1 spherulites are 1.58, 1.28, and 0.26 μm/min, respectively, at $T_c = 75$, 80, or 80 °C. By comparison, the growth rates for the embedded minority Type-2 spherulites are on

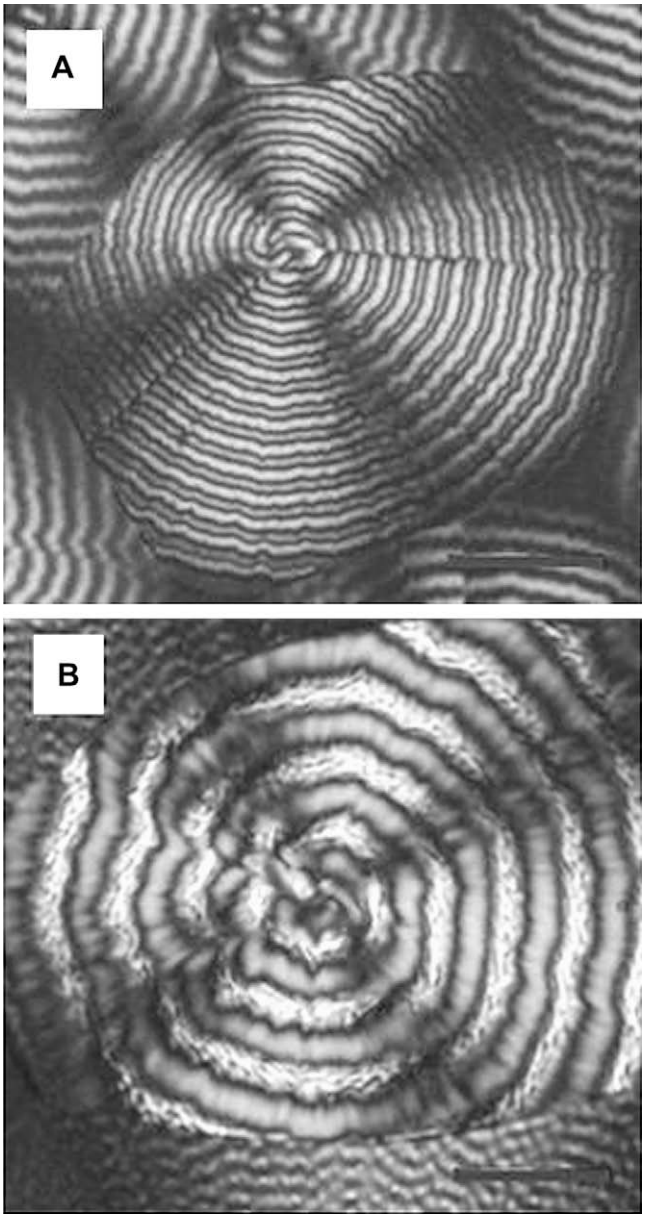

Fig. 7. POM photographs with tint plate (530 nm) for PNT samples crystallized at T_c = (A) 70 °C; (B) 80 °C. Type-2 spherulites surrounded among Type-1 spherulites, in different colors. Scale bar = 20 μm.

average about half of those for the majority Type-1 spherulites. Growth rates of the Type-2 spherulites are 0.96, 0.46, and 0.19 μm/min, respectively, at same $T_c = 75$, 80, or 80 °C.

Samples were also characterized using POM equipped with a tint plate. Fig. 7 shows POM photographs with the tint plate (530 nm) for PNT samples crystallized at two $T_c =$ (A) 70 °C; (B) 80 °C. The data show that minority Type-2 spherulites are surrounded by majority Type-1 spherulites. These two types of spherulites are apparently in different colors. In addition, the ring-bands in Type-2 spherulites are also characterized with two different alternating colors. With an increase in T_c, the inter-spacing between the double-ring bands (in Type-2) is enlarged. To reveal the difference between the morphologies of single-ring and double-ring bands, optical microscopy (OM) photographs were taken again using non-polarized light. Fig. 8 shows non-polarized light OM photos Type-0, Type-1, and Type-2 spherulites in PNT melt-crystallized at $T_c =$: (a) 45, (b) 55, (c) 60, (d) 70, and (e) 80 °C. These non-polarized light OM photographs reveal that the "double bands" actually are a crystalline band separated (spaced) by a wider band of plateau region. The single-band spherulite, on the other hand, contains the crystalline band that is roughly as wide as the plateau-band. Temperature apparently exerts a profound effect on

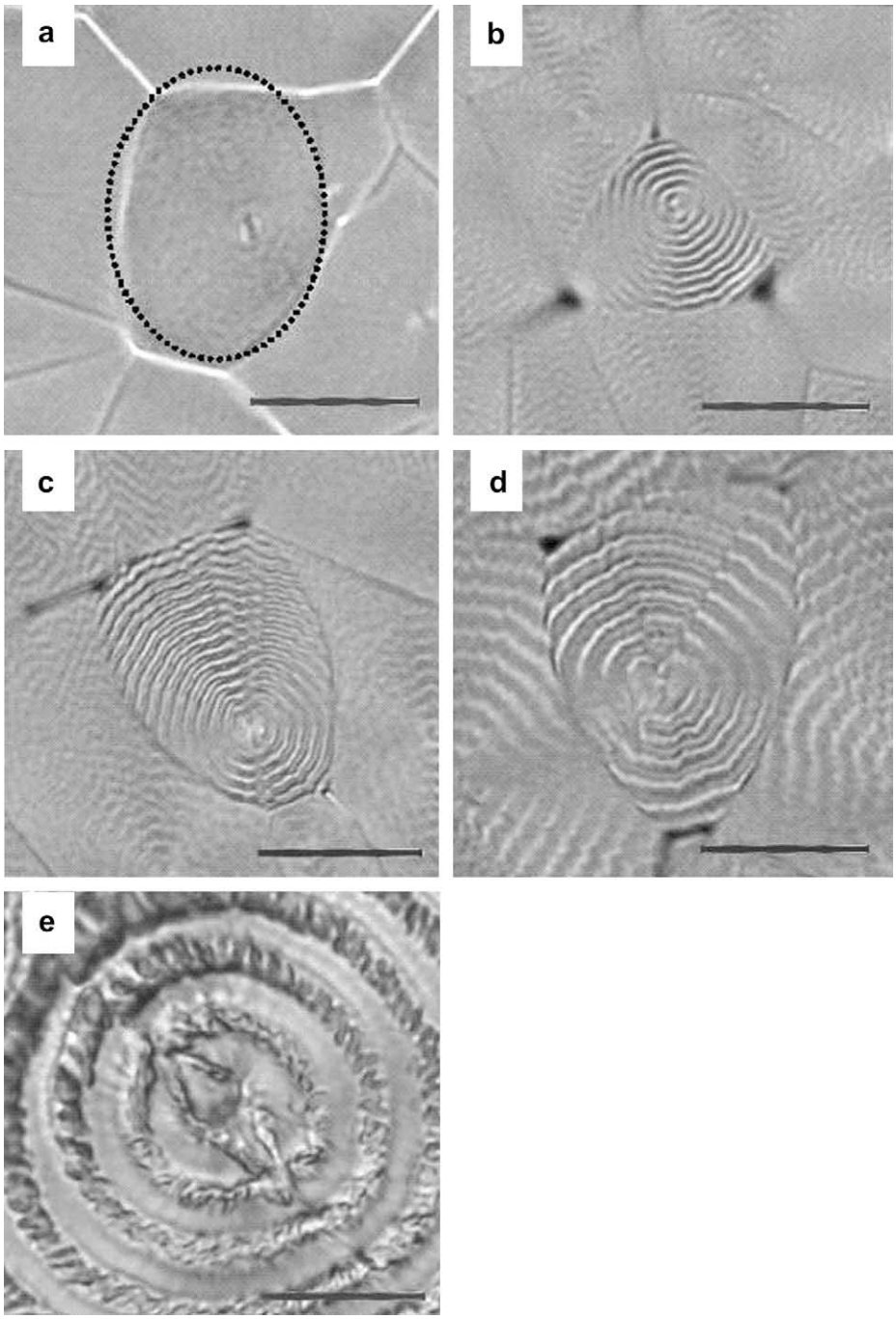

Fig. 8. Non-polarized light OM photos for melt-crystallized PNT containing Types-0, 1, or 2 spherulites grown at various T_c: (a) 45, (b) 55, (c) 60, (d) 70, and (e) 80 °C. Scale bar = 20 μm.

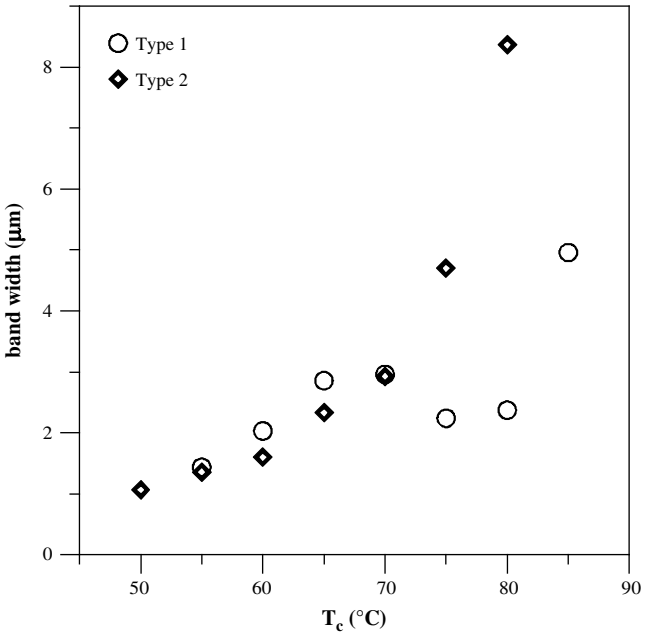

Fig. 9. Inter-band spacing of Type-1 (single band) in comparison with that of Type-2 (double band) spherulites as functions of T_c.

the patterns of spherulites in PNT. Below $T_c = 55$ °C, ringless Type-0 spherulites co-exist with double-banded Type-2 spherulites. Above $T_c = 55$ °C, the pattern is characterized with co-existing single-banded and double-banded spherulites. Greater details on lamellar crystals on the ridge vs. valley of either single-ring or double-ring bands will be shown and discussed using the SEM data in following sections.

Measurements of inter-ring spacing were taken from the non-polarized light OM photographs for the PNT samples. Band width was found to vary with temperature of crystallization for Type-1 and Type-2 spherulites in PNT. Fig. 9 shows variation of inter-band spacing (or band width) in Type-1 (single band) vs. Type-2 (double-band) spherulites grown and measured at various T_c's. Inter-ring spacings and sizes of these spherulites apparently vary with T_c. The variation trend of inter-ring spacing for both types of spherulite in PNT is summarily compared with respect to temperature of crystallization (range of 50–85 °C). With increasing temperature, the average band widths of both types slightly increase between 50 °C and 70 °C. But the inter-ring spacing for the double band spherulite (Type-2) then increases rapidly at T_c equal to or higher than 75 °C. However, the inter-ring spacing for the single-band (Type-1) spherulite reverses the trend and exhibits a dip at the same temperature (75 °C), where the inter-ring spacing for the double-band spherulite starts to increase dramatically. A reversed dip from the increasing trend occurs at $T_c = 75$ °C, which may be attributed to rapid change in the fractions of these two types of spherulites at this T_c.

3.4. Double-ring-banded (Type-2) spherulites

It is essential to reveal difference as well as origins of Type-1 (single-banded in POM) vs. minority Type-2 (double-banded in POM) spherulites. Minority here means that only a few Type-2 spherulites are found in the entire sample film (ca. 3–5 mm in diameter) on the glass slide. Furthermore, the fraction or number of the minority Type-2 spherulites does not change much with respect to T_c in range of 50–85 °C, except that lower T_c (such as 40–45 °C) does tend to result in slightly higher probability of finding the sporadic Type-2 spherulites among the majority Type-0 or Type-1 spherulites.

To inspect the differences between the spherulites of single vs. double rings in better details, larger magnification SEM characterization was performed on two PNT samples crystallized at $T_c = 70$ and 80 °C, respectively. Fig. 10 shows SEM of PNT melt-crystallized

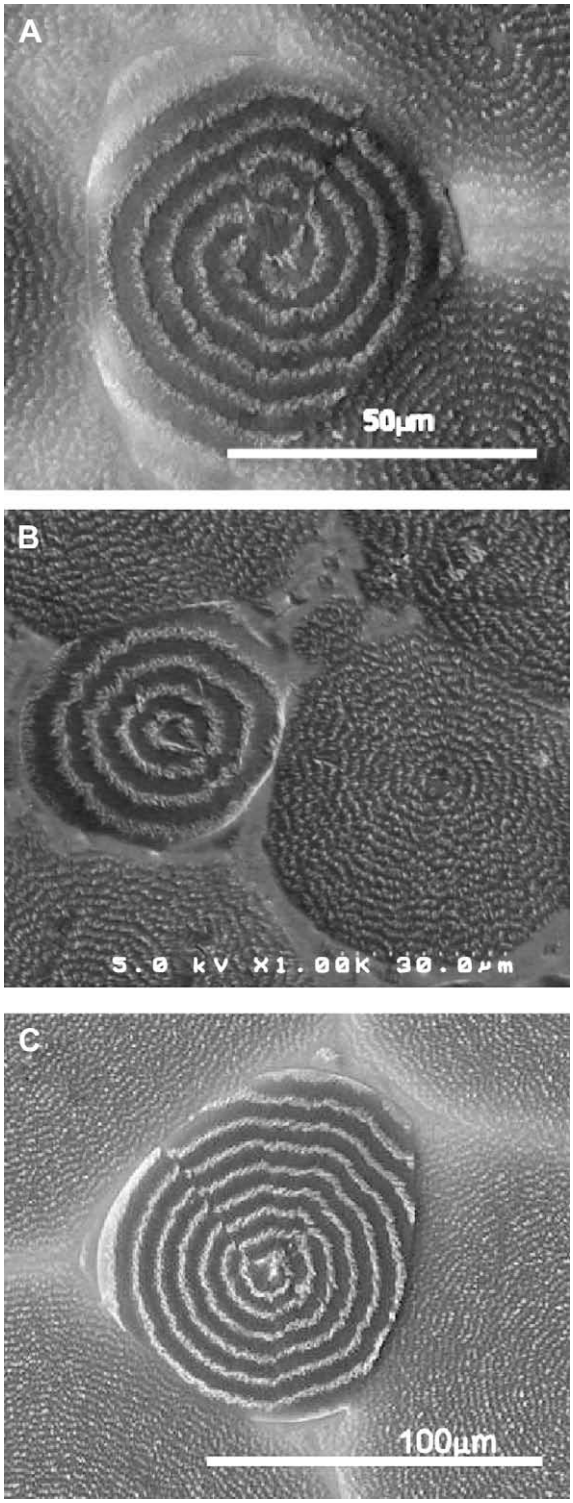

Fig. 10. SEM micrographs showing co-existing majority Type-1 and minority Type-2 spherulites in PNT melt-crystallized at (A) $T_c = 70$ °C and (B) and (C) $T_c = 80$ °C.

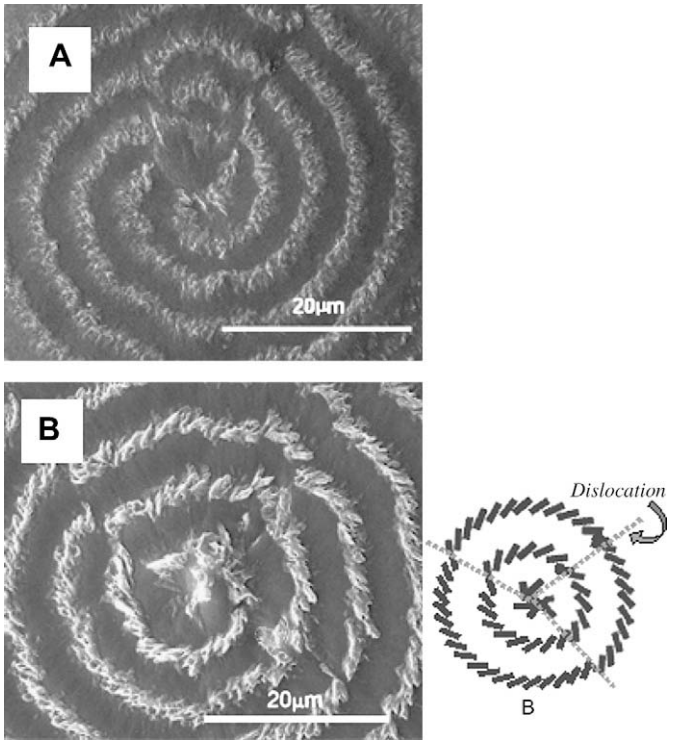

Fig. 11. Zoomed-in SEM graphs on Type-2 spherulites crystallized at (A) 70 °C, (B) 80 °C.

at $T_c = 70$ °C for (A), and 80 °C for (B) and (C). The figure shows that the SEM micrograph of PNT crystallized at higher temperatures of Regime-II ($T_c = 70$, 80 °C) reveals both majority single-ring Type-1 and the double-ring-banded Type-2 spherulites as an embedded minority species. Note that the actual relative volume fraction of Type-2 spherulites among the majority Type-1 ones is not what is apparently shown in the micrographs, since the SEM graphs were taken in such way that a single Type-2 spherulite was focused. In actual distribution, Type-1 is the predominant majority species while Type-2 spherulites are only the sporadic minority. It might be of interest to compare the difference in the inter-ring spacing of Type-1 with that of Type-2 spherulites. From the scale bars, the inter-ring band width can be estimated from these SEM photographs to be $d = 2.03$ μm for the spherulites in PNT crystallized at 80 °C. The SEM photograph (B) shows that the inter-ring spacing of double-ring spherulites is at least twice as wide as that of the single-ring spherulites (circled region). For the double-band spherulites in PNT crystallized at the same $T_c = 80$ °C, the inter-ring spacing is $d = 5.68$ μm, which is more than twice as much as that of the single-banded spherulites crystallized at the same T_c of 80 °C. These values of inter-ring spacing as estimated from the SEM photographs agree quite well with the result shown earlier in Fig. 9, where the data of inter-ring spacing have been estimated from the non-polarized light OM photographs. On average, when PNT is crystallized at the same T_c, the Type-2 spherulites (appearing as double-ring bands in POM) have larger inter-ring spacing (almost twice or three times as much) than that of the Type-1 single-band spherulites, especially at higher $T_c = 75$ or 80 °C.

The SEM photographs show much finer morphological details in the Type-2 spherulites, and the alternating ridges and inter-ring plateau, and crystalline lamellar orientation within the ring-bands are further analyzed. Fig. 11(A) and (B) shows scaled-up double-ring-banded Type-2 spherulites in PNT crystallized at 70 °C, and 80 °C, respectively. The inset of Fig. 11 shows simplified schemes of lamellar orientation on the band ridges. Zoomed-in details of Type-2 ring-bands show strikingly clear features about the crystalline ridges and flat and wide valleys in Type-2 "double-ring" bands. The bands in Type-2 spherulites, like Type-1, are mostly concentric, although occasional dislocation of the ring-bands may make the pattern appearing to be aligned in spirals originating from a nuclei center. Regardless of being concentric or seemingly spiraling, the ring-bands show vivid piles of lamellar crystals on the ridges, with the valley being featureless and flat. Especially in the Type-2 band ridges of PNT crystallized at $T_c = 80$ °C, the short rod-like crystalline aggregates (or lamellae) protrude out from the plane and they are roughly self-aligned in such way that they twist along the spiraling ridges. This is quite different from the common banding mechanisms where lamellae are proposed to twist along the radial direction during growth.

3.5. Ringless (Type-0) and single-ring-banded (Type-1) spherulites

Type-0 (at low T_c's) and Type-1 (at high T_c's) spherulites were then examined using SEM. As discussed earlier, when PNT was crystallized at lower T_c (55 °C or below), POM characterization revealed only Type-0 and Type-2 spherulites (ringless and single-ring, respectively, with the latter being sporadic minority). By contrast, when crystallized at $T_c = 55$ °C or higher, Type-1 and

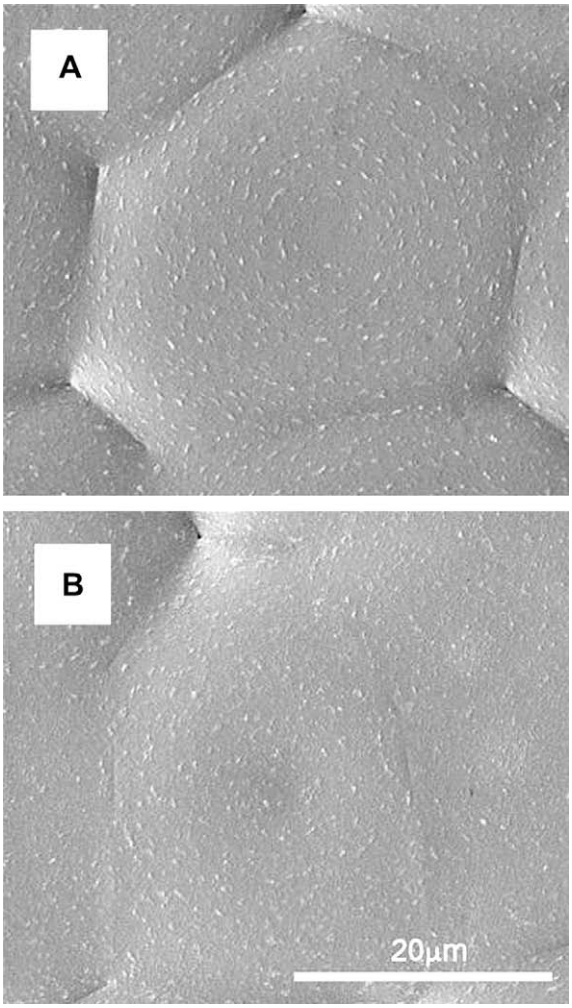

Fig. 12. SEM photos of Type-0 spherulites of PNT melt-crystallized at T_c = (A) 40 °C, (B) 50 °C.

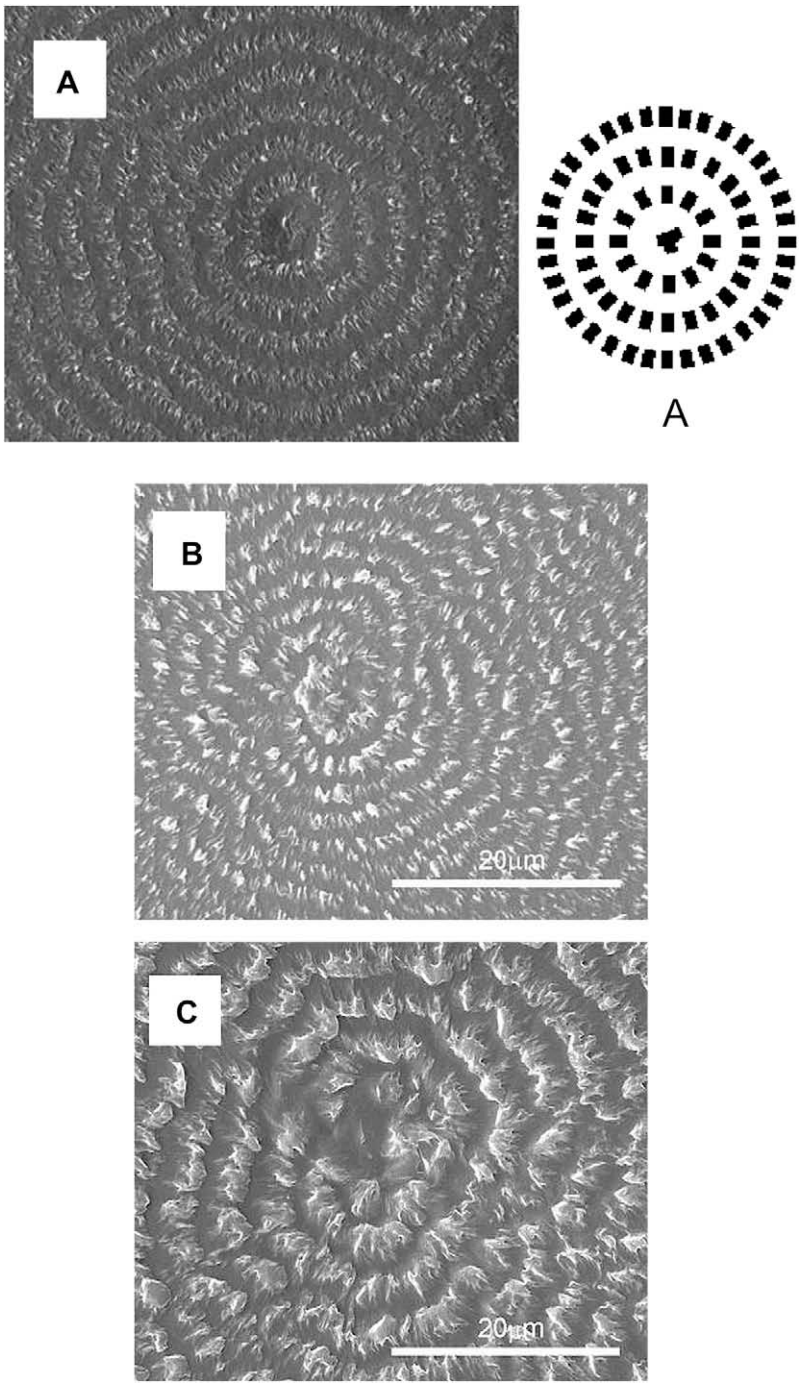

Fig. 13. SEM micrographs of Type-1 spherulites crystallized at T_c = (A) 70 °C, (B) 80 °C, and (C) 85 °C.

Type-2 spherulites (single-ring and double-ring, respectively, again with the latter being sporadic minority) were revealed in POM photographs. SEM characterization was further performed to reveal finer morphological details in the ringless Type-0 (the majority species at low T_c) and single-ring-banded Type-1 (the majority species at high T_c). Fig. 12 shows SEM photos of Type-0 spherulites of PNT melt-crystallized at lower T_c = (A) 40 °C, (B) 50 °C. Interestingly, the Type-0 spherulites, which appear ringless as viewed under POM, are really not ringless at all when viewed using SEM, as shown in Micrographs-A and -B in Fig. 12 for PNT crystallized at 40 and 50 °C, respectively. Tiny needle-like crystalline lamellae are oriented in roughly concentric circles, and note carefully also that these tiny, segmented lamellae orient themselves along the circular (viz tangential) direction rather than in the radial direction. This orientation would be somewhat difficult to interpret, as the conventional notion dictates that lamellae grow in radial direction from nuclei centers. The Type-0 spherulites may have appeared "ringless" in POM characterization due to the extremely tiny size of the regularly ordered lamellae (1 μm in length and submicron ~0.3 μm in width), which are revealed clearly in SEM micrographs as discontinuous crystal entities arranged in ring-like patterns.

Fig. 13 shows zoomed-in SEM photos specifically on Type-1 spherulites in PNT crystallized at T_c = (A) 70 °C, (B) 80 °C, and (C)

85 °C. Inset next to Photo-A shows simplified schemes of lamellar orientation on the band ridges. Note that the crystalline lamellar aggregates on the ridges of the Type-1 ring-bands are shorter than those of the Type-2 rings discussed earlier. In addition, the lamellar rods in Type-1 ring-bands are not as densely packed as those in Type-2 ones. The lamellar length in the single-ring bands (Type-1) is not quite uniform but tends to vary from about 1 to 1.5 μm. A third feature is that they do not show visible branches, turning, or twisting, either along the circular rings or toward the radial directions. The mostly circular crystalline ridges in the Type-1 ring-bands in turn are surrounded by flat valley regions, which is similar to the Type-2 ring-bands discussed earlier. For the single-band spherulites, the flat valley and the crystalline bands are in general about the same thickness; thus, magnitude of either the crystalline ring-band thickness or inter-ring spacing is roughly equal.

It would be scientifically useful to probe the nature of ring-bands by utilizing the advantages of the wide valley in Type-2 spherulites, where the clear resolution/separation between the ridges and valleys makes analysis more trustworthy. As mentioned in Introduction, one of the popular mechanisms for banding textures involves lamellar twisting, although why lamellae twist in one incidence but not in others still remains a puzzle. An interesting question may be "is there a different mechanism for banding?", especially considering the completely different and unique textures in the Type-2 spherulites.

Elemental analysis using SEM coupled with EDS apparatus was performed by focusing on the minority Type-2 spherulites. On the other hand, the Type-1 spherulites, with much narrower inter-ring spacing and less regular orientation of the crystal rods on band ridges, were considered not suitable for analysis using EDS due to likely insufficient resolution between the ridges and valleys. Fig. 14 shows EDS elemental analysis along the radial direction of a single Type-2 spherulite in PNT crystallized at 75 °C. Fig. 14(A) illustrates the corresponding positions in the Type-2 spherulites where EDS data were taken, and Graphs-B shows that the atom percents of silicon at the ridge or valley of the Type-2 ring-banded spherulite along the radial direction are shown to be up and down in going across the valley and ridge of the band. Since the electron beams can penetrate only limited depths into the PNT sample surfaces, high silicon percentages would indicate a more exposed surface that is less covered by PNT lamellae, which contain no silicon atoms. Thus, this method reveals different levels of polymer coverage (the valleys and ridges) going in radial direction in Type-2 ring-bands.

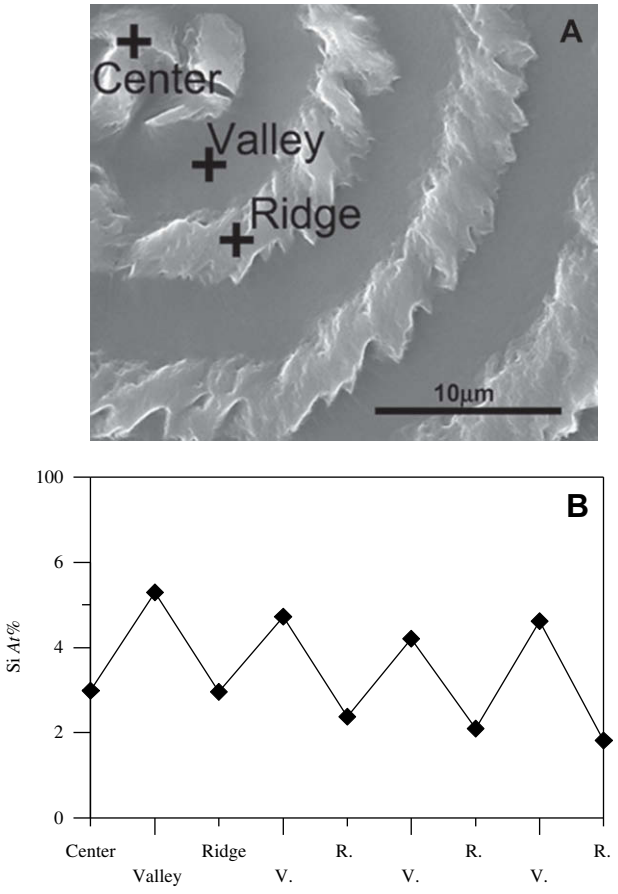

Fig. 14. Elemental analysis (EDS) result: (A) positions in spherulites where EDS data were taken on Type-2 spherulite of PNT crystallized at 75 °C, (B) Si % content measured along the radial direction.

Thus, up and down nature of film thickness along the radial direction of Type-2 spherulites is proven in EDS as well as SEM morphology characterization. However, two possibilities may account for the fact of alternating valleys and ridges in spherulites: The first possibility is that lamellar reorientation (such as spiraling, twisting, etc.) takes place in growing out in radial direction, as proposed by many investigators with numerous reports in the literature. This mechanism dictates that lamellae are continuous from center nuclei to edge of spherulites (as long as 50 μm in diameter). All lamella-bundles twist or spiral rhythmically at same intervals to form ridges (edge-on) and valleys (flat-on). In such way, polymer lamellae will cover all the time from center to edge along the radial direction without any exposed glass surface; and thus, the silicon % as revealed using EDS elemental analysis on the spherulite surface, being covered by polymer lamellar layers, should not show much difference. But as characterized using EDS, the Type-2 spherulites show significant up and down fluctuation in Si%, indicating that the plateau valley region may be likely uncovered while the ridges are covered by polymer species. For the double-ring-banded Type-2 spherulites, at least, the proposal of uninterrupted and rhythmical twisting of long lamellae may not be suitable if EDS data are considered.

The second possibility is that the crystalline rods spontaneously aggregating on ridges in such a rhythmically way to form ring-bands, with the plateau valleys being a result of either amorphous, noncrystalline species of polymer, or likely drainage of any polymer and the ridges being the crystalline part of the piled-up polymer chains. The EDS result agrees well with this possibility. It can be concluded that the formation of ring-bands of PNT Type-2 spherulites is caused by rhythmical growth of alternative ridge and valley of polymer with crystalline or noncrystalline valley region. A concurrent work in this laboratory has just discovered that similar morphology and valley-ridge textures of dual types of spherulites exist in the interior of PNT, which reveals that the growth of spherulites in three dimensions is layer by layer, packing into a multi-shells structure in 3-D ring-banded spheres [36].

4. Conclusion

A new mechanism of formation of ring-banded spherulites is proposed, where three different types of spherulites (Type-0, -1, and -2) are possible in PNT when crystallized at wide range of T_c; however, only two of the three types can co-exist in PNT crystallized at a given T_c. At lower T_c (<55 °C), the spherulites in PNT are either Type-0 (ringless in POM) or Type-2 (double-ring-banded in POM). When crystallized at temperature of $T_c = 55$ °C or higher, the morphology of PNT assumes a different pattern with Type-1 (single-ring-banded) as majority that surrounds a new Type-2 (double ring-banded) as imbedded minority. The temperature of $T_c = 55$ °C is

a point of discontinuity, where the Type-0 spherulite (ringless type) ceases to develop. Above $T_c = 55\,^{\circ}C$, the Type-1 (single-banded type) spherulite grows as the majority species with the Type-2 (double-ring-banded) pattern appearing as the minority species. Although the Type-2 spherulites would appear as the minority species at all low to high T_c range, a careful analysis revealed that the lamellar crystals would gradually thicken and the inter-ring spacing would increase with increasing T_c. At higher T_c ($>55\,^{\circ}C$), all spherulites in PNT are ring-banded; however, the ring-banded spherulites are composed of majority spherulites being single-banded (Type-1) and minority being double-banded (Type-2). The relative fraction of Type-1 to Type-2 spherulites in PNT depends on T_c, with the higher T_c the less growth of Type-2 spherulites.

As revealed in SEM, Type-1 and Type-2 (single- or double-ring, respectively, in POM), are both ring-banded spherulites which differ distinctly in the inter-ring spacing as well as in the order of orientation of the lamellar crystals on the ridges (summits) of ring-bands. The valley (flat region) in Type-2 ring band is wide enough to appear as an extra optical ring, which makes it double-ring-banded in POM. On the other hand, Type-0 spherulite is not really ringless; and the ultra-tiny grainy crystals in Type-0 spherulites as revealed in SEM would appear as "ringless" in POM. That is, the terms of single-ring and double-ring for Type-1 and Type-2, respectively, are terminology as far as optical properties are only concerned. The phenomenon of double rings in POM images actually is a result of increased spacing between the crystalline bands, where the wider plateau forms an additional optical "band".

There are finer morphological differences among the PNT spherulites showing ringless, single-band, or double-band patterns in POM. The concentric rings in double-band spherulites (Type-2) have much larger inter-ring spacing ($d = 5.68\,\mu m$) than do the single-rings in single-band spherulites ($d = 2.03\,\mu m$). In general, the inter-ring spacing for the single-ring spherulites is one half or less that for double-banded spherulites in PNT when crystallized at the same T_c. By comparison, the rod-like lamellae in the double-banded spherulites (Type-2) are longer and thicker, and more ordered than those in the single-banded spherulites (Type-1). Alignment of the rod-like lamellae in Type-2 spherulites tends to tilt more orderly toward a same angle away from radial direction; on the other hand, alignment of the rods in Type-1 spherulites is less orderly, but roughly tilts toward the radial direction. The lamellar rods are packed in patterns that form concentric rings with occasional dislocation that more or less coincides with optical Maltese-cross. The dislocation of rods' alignment can make the rings occasionally offset to appear spiral rather than concentric.

Acknowledgments

This work was financially supported by basic research grants in three consecutive years (NSC-94 2216 E006 003) and (NSC 96-2221-E-006-099-MY3) funded by *National Science Council* (NSC) of Taiwan. A part of SEM results used in this study was performed with assistance by Department of Nanostructure and Advanced Materials, Kagoshima University, Kagoshima, Japan, via international collaboration/exchange funding kindly provided by Prof. Y. Suda of Venture Business Laboratory (VBL) at Kagoshima University.

References

[1] Keith HD, Padden Jr FJ. Polymer 1984;25:28.
[2] Lovinger AJ, Keith HD. Macromolecules 1996;29:8541.
[3] Keith HD, Padden Jr FJ. Macromolecules 1996;29:7776.
[4] Keller A. J Polym Sci Polym Phys 1955;17:291.
[5] Wang J, Lin CY, Hanzlicek J, Cheng SZD, Geil PH, Grebowicz J, et al. Polymer 2001;42:7171.
[6] Hu YS, Liu RYF, Zhang LQ, Rogunova M, Schiraldi DA, Nazarenko S, et al. Macromolecules 2002;35:7326.
[7] Wang Z, An L, Jiang W, Jiang B, Wang X. J Polym Sci Polym Phys 1999;37:2682.
[8] Keith HD. Macromolecules 1982;15:114.
[9] Keith HD, Padden Jr FJ, Russell TP. Macromolecules 1989;22:666.
[10] Lotz B, Thierry A. Macromolecules 2003;36:286.
[11] Woo EM, Wu PL. Colloid Polym Sci 2006;284:357.
[12] Woo EM, Wu PL, Wu MC, Yen KC. Macromol Chem Phys 2006;207:2232.
[13] Wu PL, Woo EM. J Polym Sci Polym Phys 2004;42:1265.
[14] Yasuniwa M, Tsubakihara S, Iura K, Ono Y, Dan Y, Takahashi K. Polymer 2006;47:7554.
[15] Okabe Y, Kyu T, Saito H, Inoue T. Macromolecules 1998;31:5823.
[16] Jiang Y, Zhou JJ, Li L. Langmuir 2003;19:7417.
[17] Hobbs JK, Binger DR, Keller A, Barham PJ. J Polym Sci Polym Phys 2000;38:1575.
[18] Hoffman JD, Miller RL. Macromolecules 1988;21:3038.
[19] Wang Y, Chan CM, Li L, Ng KM. Langmuir 2006;22:7384.
[20] Xu J, Guo BH, Zhang ZM, Zhou JJ, Jiang Y, Yan S, et al. Macromolecules 2004;37:4118.
[21] Beekmans LGM, Hempenius MA, Vancso GJ. Eur Polym J 2004;40:893.
[22] Chuang WT, Hong PD, Chuah HH. Polymer 2004;45:2413.
[23] Singfield KL, Hobbs JK, Keller A. J Cryst Growth 1998;183:683.
[24] Lotz B, Cheng SZD. Polymer 2005;46:577.
[25] Duan Y, Zhang Y, Yan S, Schultz JM. Polymer 2005;46:9015.
[26] Frömsdorf A, Woo EM, Lee LT, Chen YF, Förster S. Macromol Rapid Commun 2008;29:1322.
[27] Wang Z, Hu Z, Chen Y, Gong Y, Huang H, He T. Macromolecules 2007;40:4381.
[28] Wang Z, Alfonso GC, Hu Z, Zhang J, He T. Macromolecules 2008;41:7584.
[29] Maillard D, Prud'homme RE. Macromolecules 2008;41:1705.
[30] Chen J, Yang D. Macromolecules 2005;38:3371.
[31] Cheung ZL, Weng LT, Chan CM, Hou WM, Li L. Langmuir 2005;21:7968.
[32] Geil PH. Polymer single crystals. Huntington, NY: Robert E. Krieger Pub; 1973.
[33] Murayama E. Polym Prepr Jpn 2002;51:460.
[34] Chen YF, Woo EM, Li SH. Langmuir 2008;24:11880.
[35] Hoffman JD, Davis GT, Lauritzen JI. In: Hannay NB, editor. Treatise on solid state chemistry, vol. 3. New York: Plenum; 1976 [chapter 7].
[36] Chen YF, Woo EM. Macromol Rapid Commun, in press.